



**HAL**  
open science

## Measuring absolute spin polarization in dissolution-DNP by Spin Polarimetry Magnetic Resonance (SPY-MR).

Basile Vuichoud, Jonas Milani, Quentin Chappuis, Aurélien Bornet, Geoffrey Bodenhausen, Sami Jannin

► **To cite this version:**

Basile Vuichoud, Jonas Milani, Quentin Chappuis, Aurélien Bornet, Geoffrey Bodenhausen, et al.. Measuring absolute spin polarization in dissolution-DNP by Spin Polarimetry Magnetic Resonance (SPY-MR).. Journal of Magnetic Resonance, 2015, 260, pp.127-135. 10.1016/j.jmr.2015.09.006 . hal-01255407

**HAL Id: hal-01255407**

**<https://hal.science/hal-01255407>**

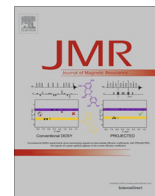
Submitted on 8 Dec 2016

**HAL** is a multi-disciplinary open access archive for the deposit and dissemination of scientific research documents, whether they are published or not. The documents may come from teaching and research institutions in France or abroad, or from public or private research centers.

L'archive ouverte pluridisciplinaire **HAL**, est destinée au dépôt et à la diffusion de documents scientifiques de niveau recherche, publiés ou non, émanant des établissements d'enseignement et de recherche français ou étrangers, des laboratoires publics ou privés.



Distributed under a Creative Commons Attribution - NonCommercial - NoDerivatives 4.0 International License



## Measuring absolute spin polarization in dissolution-DNP by Spin Polarimetry Magnetic Resonance (SPY-MR)



Basile Vuichoud<sup>a,\*</sup>, Jonas Milani<sup>a</sup>, Quentin Chappuis<sup>a</sup>, Aurélien Bornet<sup>a</sup>, Geoffrey Bodenhausen<sup>a,b,c,d</sup>, Sami Jannin<sup>a,e,\*</sup>

<sup>a</sup> Institut des Sciences et Ingénierie Chimiques, Ecole Polytechnique Fédérale de Lausanne, 1015 Lausanne, Switzerland

<sup>b</sup> Ecole Normale Supérieure-PSL Research University, Département de Chimie, 24 rue Lhomond, 75005 Paris, France

<sup>c</sup> Sorbonne Universités, UPMC Paris 06, LBM, 4 place Jussieu, 75005 Paris, France

<sup>d</sup> CNRS, UMR 7203 LBM, 75005 Paris, France

<sup>e</sup> Bruker BioSpin AG, Industriestrasse 26, 8117 Fällanden, Switzerland

### ARTICLE INFO

#### Article history:

Received 29 July 2015

Revised 10 September 2015

Available online 25 September 2015

Dedicated to Stefan Schäublin, Alfred Höhener and Richard Ernst for their pioneering work.

#### Keywords:

NMR spectroscopy

Dissolution Dynamic Nuclear Polarization

Spin spin

Spin temperature

Hyperpolarization

Direct measurement of polarization

### ABSTRACT

Dynamic nuclear polarization at 1.2 K and 6.7 T allows one to achieve spin temperatures on the order of a few millikelvin, so that the high-temperature approximation ( $\Delta E < kT$ ) is violated for the nuclear Zeeman interaction  $\Delta E = \gamma B_0 \hbar / (2\pi)$  of most isotopes. Provided that, after rapid dissolution and transfer to an NMR or MRI system, the hyperpolarized molecules contain at least two nuclear spins  $I$  and  $S$  with a scalar coupling  $J_{IS}$ , the polarization of spin  $I$  (short for 'investigated') can be determined from the asymmetry  $A_S$  of the multiplet of spin  $S$  (short for 'spy'), provided perturbations due to second-order (strong coupling) effects are properly taken into account. If spin  $S$  is suitably discreet and does not affect the relaxation of spin  $I$ , this provides an elegant way of measuring spin polarizations 'on the fly' in a broad range of molecules, thus obviating the need for laborious measurements of signal intensities at thermal equilibrium. The method, dubbed Spin Polarimetry Magnetic Resonance (SPY-MR), is illustrated for various pairs of  $^{13}\text{C}$  spins ( $I, S$ ) in acetate and pyruvate.

© 2015 The Authors. Published by Elsevier Inc. This is an open access article under the CC BY-NC-ND license (<http://creativecommons.org/licenses/by-nc-nd/4.0/>).

### 1. Introduction

Dissolution Dynamic Nuclear Polarization (D-DNP) is a technique of choice for increasing the sensitivity of magnetic resonance by up to 5 orders of magnitude [1]. The nuclear polarization can be increased by saturating the ESR transitions of polarizing agents such as TEMPOL (4-hydroxy-2,2,6,6-tetramethylpiperidin-1-oxyl) at low temperatures and moderate magnetic fields (in many laboratories at  $T = 1.2$  K and  $B_0 = 3.35$  T). We have recently shown that the polarization of protons could be boosted to  $P(^1\text{H}) > 90\%$  in a field of  $B_0 = 6.7$  T, and that cross-polarization (CP) [2,3] from  $^1\text{H}$  to  $^{13}\text{C}$  could yield unprecedented polarizations  $P(^{13}\text{C}) > 70\%$  with remarkably short build-up times  $\tau_{\text{CP-DNP}} < 10$  min [4–7]. Such a

$^{13}\text{C}$  polarization corresponds to a spin temperature  $T_{\text{spin}}(^{13}\text{C}) < 2$  mK. The DNP samples can be rapidly dissolved and transferred to an NMR or MRI system for observation, while preserving most of the polarization [7].

One of the practical challenges of D-DNP is the accurate determination of the nuclear spin polarization  $P(^{13}\text{C})$ , or, equivalently, of the spin temperature  $T_{\text{spin}}(^{13}\text{C})$ . This is usually done by comparing signals obtained with and without DNP at low temperature (typically 4.2 or 1.2 K) prior to dissolution, then again in the liquid state at room temperature immediately after dissolution, and finally at thermal equilibrium (TE) after complete relaxation. However, when a hyperpolarized substance is injected into a living organism, e.g., for real-time metabolic imaging [8,9], or more generally in any experiment where the hyperpolarized substance is diluted or undergoes irreversible biochemical transformations, the measurement of a thermal equilibrium signal can be difficult or even impossible.

It has recently been shown that in the liquid state after hyperpolarization by dissolution-DNP, the strong polarization of a nuclear spin (here noted  $^{13}\text{C}^I$  or simply  $I$  for 'investigated' spin)

**Abbreviations:** D-DNP, Dissolution-Dynamic Nuclear Polarization; TEMPOL, 4-hydroxy-2,2,6,6-tetramethylpiperidin-1-oxyl; CP, Hartmann–Hahn Cross-Polarization.

\* Corresponding authors.

**E-mail addresses:** [basile.vuichoud@epfl.ch](mailto:basile.vuichoud@epfl.ch) (B. Vuichoud), [sami.jannin@epfl.ch](mailto:sami.jannin@epfl.ch) (S. Jannin).

**URLs:** <http://lrm.epfl.ch> (B. Vuichoud), <http://lrm.epfl.ch> (S. Jannin).

<http://dx.doi.org/10.1016/j.jmr.2015.09.006>

1090-7807/© 2015 The Authors. Published by Elsevier Inc.

This is an open access article under the CC BY-NC-ND license (<http://creativecommons.org/licenses/by-nc-nd/4.0/>).

leads to an asymmetry  $A_S$  of the multiplet of a neighboring spin [10–14], with some restrictions that we shall discuss below, this feature can in principle be used for a broad range of homo- or heteronuclear scalar-coupled spin systems, and provides an elegant way to measure spin polarizations ‘on the fly’ while obviating the need for laborious measurements of signal intensities at thermal equilibrium. It is worth noticing that these observations are reminiscent of previous work related to solid samples at low temperatures [15–18] in some cases enhanced by DNP [19–21]. Moreover, Donovan et al. [22] have shown that rapid heteronuclear cross-relaxation could lead to a significant transfer of magnetization. This is a case where the use of SPY-MR cannot be recommended.

In this work, we propose a simple theoretical explanation for this effect and discuss its limitations. We show that the method is reliable, provided (i) DNP leads to a uniform spin temperature in the  $^{13}\text{C}$  nuclear spin reservoir in the frozen solid (which normally occurs through spin diffusion); (ii) the cross-relaxation and cross-correlation rates that describe the coupling between Zeeman polarization and two-spin order after dissolution can be neglected, a condition that is often fulfilled since cross-terms between the chemical shift anisotropy and the dipole–dipole couplings between spins  $I$  and  $S$  are typically small; (iii) that effects of second-order coupling on the intensities of multiplets (“strong coupling” or “roof effect”) are properly taken into account. We call the method Spin PolarimetrY for Magnetic Resonance (SPY-MR) and we shall illustrate it for several  $I, S$  spin pairs  $^{13}\text{C}^I, ^{13}\text{C}^S$  in acetate and pyruvate.

### 1.1. Traditional determination of the polarization

In practice, in our polarizer operating at 6.7 T and 1.2 or 4.2 K [6,7] the DNP build-up of  $P(^{13}\text{C})$  can be measured by applying small nutation angle  $rf$  pulses (typically  $\beta^{\text{small}} = 5^\circ$  so as to limit perturbation of the polarization) at regular time intervals (usually  $\Delta t = 5$  s). Before starting the DNP experiment, i.e., before applying the microwave field, the sample must be left for a long time  $t \gg 5T_1(^{13}\text{C})$  at 1.2 or 4.2 K in order to let the polarization fully relax to its Boltzmann equilibrium. The resulting signal in thermal equilibrium  $I_{\text{TE}}(^{13}\text{C})$  can in principle be measured by applying a single  $rf$  pulse with a  $\beta = 90^\circ$  nutation angle, but we prefer to perform  $N$  acquisitions at intervals  $\Delta t^{\text{TE}} \ll 5T_1(^{13}\text{C})$  with the same pulse  $\beta^{\text{small}}$  to prevent calibration errors. The resulting sum of signals needs to be normalized by dividing by the factor  $\delta$ :

$$\delta = \sum_{i=1}^N (\cos \beta^{\text{small}})^{i-1} \quad (1)$$

to account for the number of scans  $N$  and the increasing depletion of the polarization caused by the train of pulses, neglecting  $T_1(^{13}\text{C})$  relaxation in the pulse intervals. The integral of the thermal equilibrium signal at 1.2 or 4.2 K will be noted  $I_{\text{TE}}(^{13}\text{C})$ . The thermal equilibrium polarization is determined by Boltzmann’s law:

$$P_{\text{TE}}(^{13}\text{C}) = \tanh\left(\frac{\hbar\omega}{2k_B T}\right) \quad (2)$$

which amounts to  $P_{\text{TE}}(^{13}\text{C}) = 0.143\%$  at 6.7 T and 1.2 K, or 0.0409% at 6.7 T and 4.2 K. After the microwave field is switched on, the integral  $I_{\text{DNP}}(^{13}\text{C})$  of the spectrum enhanced by DNP is usually measured with a single pulse of same nutation angle  $\beta^{\text{small}} = 5^\circ$ . The enhanced polarization is obtained from the ratio:

$$\epsilon_{\text{DNP}} = \frac{P_{\text{DNP}}(^{13}\text{C})}{P_{\text{TE}}(^{13}\text{C})} = \delta \cdot \frac{I_{\text{DNP}}(^{13}\text{C})}{I_{\text{TE}}(^{13}\text{C})} \quad (3)$$

where  $\delta$  is defined in Eq. (1). After dissolution, the polarization levels are usually measured in a similar way by comparing the

hyperpolarized  $^{13}\text{C}$  polarization  $P_{\text{DNP}}(^{13}\text{C})$  observed immediately after dissolution with the thermal polarization  $P_{\text{TE}}(^{13}\text{C})$  observed once the hyperpolarization has completely decayed to Boltzmann equilibrium. This must be done after a prolonged delay of at least  $t = 16T_1(^{13}\text{C})$ , bearing in mind that, if one starts with an enhancement  $\epsilon = 10^5$ , the factor  $\exp(-t/T_1(^{13}\text{C})) = e^{-16} = 1.1 \cdot 10^{-7}$  merely allows one to approach thermal equilibrium within 1%. At ambient temperature  $T = 300$  K and  $B_0 = 7$  T (300 MHz for protons), the Boltzmann thermal equilibrium polarization is  $P_{\text{TE}}(^{13}\text{C}) = 6.02 \cdot 10^{-6}$ . The thermal equilibrium signal can be measured by applying  $rf$  pulses with  $90^\circ$  nutation angles spaced by  $5T_1$ , i.e., typically every 5 min for  $^{13}\text{C}$  nuclei with long  $T_1$ . For molecules that are isotopically enriched in  $^{13}\text{C}$  with concentrations in the millimolar range, 128 transients are typically needed to achieve a sufficient signal-to-noise ratio at 300 MHz without cryoprobe, which can require about 10 h. Thus the laborious observation of a reference  $^{13}\text{C}$  signal to determine the thermal polarization  $P_{\text{TE}}(^{13}\text{C})$  can actually require more time than the dissolution experiment itself! With our equipment, measurements of  $P_{\text{TE}}(^{13}\text{C})$  are virtually impossible for molecules in natural abundance.

## 2. Asymmetry of doublets for non-equilibrium populations

### 2.1. Energy levels and polarizations in a coupled two-spin system with $\gamma_I > 0, \gamma_S > 0, J_{IS} > 0$ , and $|v_S| > |v_I|$

Fig. 1 shows the energy diagram of a two-spin system in isotropic solution with a scalar coupling constant  $J_{IS} > 0$  and a difference

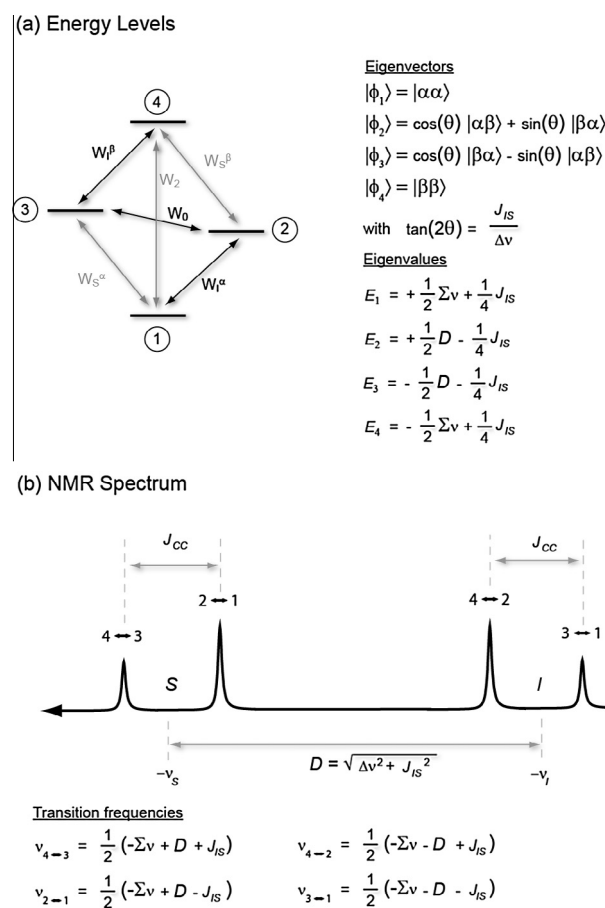


Fig. 1. (a) Energy diagram of a strongly scalar coupled homonuclear two-spin system with  $\gamma_I > 0, \gamma_S > 0$  and  $J_{IS} > 0$  and (b) its corresponding NMR spectrum at thermal equilibrium.

in chemical shifts  $\Delta\nu = \nu_I - \nu_S$ , where  $\nu_I = -\gamma_I(1 - \sigma_I)B_0$  and  $\nu_S = -\gamma_S(1 - \sigma_S)B_0$  are the Larmor frequencies of spins  $I$  and  $S$ . Note that in the usual notation,  $\nu_I$  and  $\nu_S$  have opposite signs compared to  $\gamma_I$  and  $\gamma_S$ , so that both frequencies are negative for a pair of  $^{13}\text{C}$  nuclei. This case is illustrated by the examples of singly labeled sodium pyruvate- $d_3$  [ $\text{CD}_3\text{CO}^{13}\text{COO}^- \text{Na}^+$ ] and doubly labeled sodium acetate- $d_3$  [ $^{13}\text{CD}_3^{13}\text{COO}^- \text{Na}^+$ ]. Other cases will be discussed below.

## 2.2. Eigenstates of a coupled two-spin system

In the general case of a pair of  $J$ -coupled spins  $1/2$ , the familiar spin Hamiltonian in the rotating frame is

$$\mathcal{H} = \nu_I I_z + \nu_S S_z + J_{IS} \mathbf{I} \mathbf{S} \quad (4)$$

This Hamiltonian can be represented as a matrix in the Zeeman product basis  $\{|\alpha\alpha\rangle, |\alpha\beta\rangle, |\beta\alpha\rangle, |\beta\beta\rangle\}$

$$\mathcal{H} = \frac{1}{2} \begin{pmatrix} \Sigma\nu + \frac{1}{2}J_{IS} & 0 & 0 & 0 \\ 0 & \Delta\nu - \frac{1}{2}J_{IS} & J_{IS} & 0 \\ 0 & J_{IS} & -\Delta\nu - \frac{1}{2}J_{IS} & 0 \\ 0 & 0 & 0 & -\Sigma\nu + \frac{1}{2}J_{IS} \end{pmatrix} \quad (5)$$

where  $\Sigma\nu = \nu_I + \nu_S$  and  $\Delta\nu = \nu_I - \nu_S$  are the sum and difference of the Larmor frequencies of  $I$  and  $S$  in units of Hz. Note that  $\Sigma\nu < 0$  in our example where  $\gamma_I$  and  $\gamma_S > 0$ . The eigenstates of the strongly coupled two spin “AB” system can be determined by standard methods:

$$\begin{aligned} |\phi_1\rangle &= \begin{pmatrix} 1 \\ 0 \\ 0 \\ 0 \end{pmatrix} \\ |\phi_2\rangle &= \begin{pmatrix} 0 \\ \cos\theta \\ \sin\theta \\ 0 \end{pmatrix} \\ |\phi_3\rangle &= \begin{pmatrix} 0 \\ -\sin\theta \\ \cos\theta \\ 0 \end{pmatrix} \\ |\phi_4\rangle &= \begin{pmatrix} 0 \\ 0 \\ 0 \\ 1 \end{pmatrix} \end{aligned} \quad (6)$$

where the angle  $\theta$  expresses the strength of the coupling and is defined by

$$\tan 2\theta = \frac{J_{IS}}{\Delta\nu} \quad (7)$$

Heteronuclear systems are always weakly coupled ( $\sin 2\theta \approx 0$ ) in the laboratory frame since  $J_{IS} \ll \Delta\nu$ . In homonuclear systems where  $\gamma_I = \gamma_S$ , the sign of  $\theta$  depends on the signs of  $J_{IS}$  and of  $\Delta\nu$ . Note that  $\Delta\nu > 0$  in our example where  $|\nu_S| > |\nu_I|$ . The associated eigenvalues are

$$\begin{aligned} E_1 &= \frac{1}{2}\Sigma\nu + \frac{1}{4}J_{IS} \\ E_2 &= +\frac{1}{2}D - \frac{1}{4}J_{IS} \\ E_3 &= -\frac{1}{2}D - \frac{1}{4}J_{IS} \\ E_4 &= -\frac{1}{2}\Sigma\nu + \frac{1}{4}J_{IS} \end{aligned} \quad (8)$$

with  $D = \sqrt{\Delta\nu^2 + J_{IS}^2}$

## 2.3. Transition frequencies and amplitudes

The transition frequencies of the coupled two-spin system correspond to

$$\begin{aligned} \nu_{4 \leftarrow 3} &= \frac{1}{2}(-\Sigma\nu + D + J_{IS}) \\ \nu_{2 \leftarrow 1} &= \frac{1}{2}(-\Sigma\nu + D - J_{IS}) \\ \nu_{4 \leftarrow 2} &= \frac{1}{2}(-\Sigma\nu - D + J_{IS}) \\ \nu_{3 \leftarrow 1} &= \frac{1}{2}(-\Sigma\nu - D - J_{IS}) \end{aligned} \quad (9)$$

where  $-\Sigma\nu > 0$  in our example. The intensities of the four lines depend on the populations of the four levels just before the  $rf$  pulse. If the high-temperature approximation is fulfilled for the nuclear Zeeman interaction, i.e. if  $kT \gg \Delta E = \hbar\gamma B_0$ , and bearing in mind that the unity operator  $\hat{E}$  does not affect the outcome of experiments, the density operator at thermal equilibrium can be written

$$\rho_{TE} \propto I_z + S_z \quad (10)$$

Specifically, at  $T = 300$  K and  $B_0 = 7.05$  T

$$\begin{aligned} \rho_{TE} &= \frac{1}{2} \left\{ 6.03 \times 10^{-6} \cdot I_z + 6.03 \times 10^{-6} \cdot S_z + 36.36 \times 10^{-12} \cdot 2I_z S_z \right. \\ &\quad \left. + 0.5 \cdot \hat{E} \right\} \cong 3.015 \times 10^{-6} (I_z + S_z) + 0.25 \cdot \hat{E} \end{aligned} \quad (11)$$

If one starts with populations at thermal equilibrium (or, more generally, if the high temperature approximation is fulfilled, and if the two spins  $I$  and  $S$  have a common spin temperature), the intensities of the four lines give rise to the typical “roof effect”, the inner lines having intensities  $a_{4 \leftarrow 2} = a_{2 \leftarrow 1}$  that are proportional to  $(1 + \sin 2\theta)$ , the outer lines  $a_{3 \leftarrow 1} = a_{4 \leftarrow 3}$  being proportional to  $(1 - \sin 2\theta)$ .

On the other hand, if the four populations are distributed in an arbitrary manner, in particular in hyperpolarized systems where the high temperature approximation is violated, one has to define a density operator:

$$\rho = n_1 |\phi_1\rangle\langle\phi_1| + n_2 |\phi_2\rangle\langle\phi_2| + n_3 |\phi_3\rangle\langle\phi_3| + n_4 |\phi_4\rangle\langle\phi_4| \quad (12)$$

where  $n_1, n_2, n_3$ , and  $n_4$  are the populations associated with the four eigenstates  $|\phi_1\rangle, |\phi_2\rangle, |\phi_3\rangle$ , and  $|\phi_4\rangle$ .

## 2.4. Signal amplitudes as a function of the populations

After a pulse with an arbitrary nutation angle  $\beta$  the signal amplitudes can readily be calculated [23]:

$$\begin{aligned} a_{4 \leftarrow 3} &= -\frac{1}{2} \sin\beta \left( \sin^2 \frac{\beta}{2} (1 - \sin 2\theta)(n_3 - n_1) \right. \\ &\quad \left. - \sin^2 \frac{\beta}{2} \cos^2 2\theta (n_3 - n_2) + \cos^2 \frac{\beta}{2} (1 - \sin 2\theta)(n_4 - n_3) \right) \\ a_{2 \leftarrow 1} &= -\frac{1}{2} \sin\beta \left( \cos^2 \frac{\beta}{2} (1 + \sin 2\theta)(n_2 - n_1) \right. \\ &\quad \left. - \sin^2 \frac{\beta}{2} \cos^2 2\theta (n_3 - n_2) + \sin^2 \frac{\beta}{2} (1 + \sin 2\theta)(n_4 - n_2) \right) \\ a_{4 \leftarrow 2} &= -\frac{1}{2} \sin\beta \left( \sin^2 \frac{\beta}{2} (1 + \sin 2\theta)(n_2 - n_1) \right. \\ &\quad \left. + \sin^2 \frac{\beta}{2} \cos^2 2\theta (n_3 - n_2) + \cos^2 \frac{\beta}{2} (1 + \sin 2\theta)(n_4 - n_2) \right) \\ a_{3 \leftarrow 1} &= -\frac{1}{2} \sin\beta \left( \cos^2 \frac{\beta}{2} (1 - \sin 2\theta)(n_3 - n_1) \right. \\ &\quad \left. + \sin^2 \frac{\beta}{2} \cos^2 2\theta (n_3 - n_2) + \sin^2 \frac{\beta}{2} (1 - \sin 2\theta)(n_4 - n_3) \right) \end{aligned} \quad (13)$$

The two Zeeman polarizations and the longitudinal two-spin order term can be defined as normalized expectation values expressed as a function of the four populations  $n_1, n_2, n_3$ , and  $n_4$  in the eigen basis:

$$\begin{aligned} P(I_z) &= 2 \frac{\text{Tr}(\rho I_z)}{\text{Tr}(\rho)} = (n_1 - n_4) + (n_2 - n_3) \cos 2\theta \\ P(S_z) &= 2 \frac{\text{Tr}(\rho S_z)}{\text{Tr}(\rho)} = (n_1 - n_4) + (n_3 - n_2) \cos 2\theta \\ P(2I_z S_z) &= 2 \frac{\text{Tr}(\rho 2I_z S_z)}{\text{Tr}(\rho)} = (n_1 - n_2) - (n_3 - n_4) \end{aligned} \quad (14)$$

Or, the other way around, the four populations  $n_1, n_2, n_3$ , and  $n_4$  can be expressed as linear combinations of the two Zeeman polarizations and the longitudinal two-spin order term:

$$\begin{aligned} n_1 &= \frac{1}{4}(1 + P(I_z) + P(S_z) + P(2I_z S_z)) \\ n_2 &= \frac{1}{4} \left( 1 - P(2I_z S_z) + (P(I_z) - P(S_z)) \frac{1}{\cos 2\theta} \right) \\ n_3 &= \frac{1}{4} \left( 1 - P(2I_z S_z) + (P(S_z) - P(I_z)) \frac{1}{\cos 2\theta} \right) \\ n_4 &= \frac{1}{4}(1 - P(I_z) - P(S_z) + P(2I_z S_z)) \end{aligned} \quad (15)$$

Hence one can describe the four signal amplitudes in Fig. 1 as a function of the two Zeeman polarizations and the longitudinal two-spin order term

$$\begin{aligned} a_{4 \rightarrow 3} &= \frac{1}{8} \sin \beta (1 - \sin 2\theta) \left( 2 \frac{P(S_z) \cos \theta - P(I_z) \sin \theta}{\cos \theta - \sin \theta} \right. \\ &\quad \left. - \cos \beta (2P(2I_z S_z) + (P(S_z) - P(I_z)) \tan 2\theta) \right) \\ a_{2 \rightarrow 1} &= \frac{1}{8} \sin \beta (1 + \sin 2\theta) \left( 2 \frac{P(S_z) \cos \theta + P(I_z) \sin \theta}{\cos \theta + \sin \theta} \right. \\ &\quad \left. + \cos \beta (2P(2I_z S_z) + (P(S_z) - P(I_z)) \tan 2\theta) \right) \\ a_{4 \rightarrow 2} &= \frac{1}{8} \sin \beta (1 + \sin 2\theta) \left( 2 \frac{P(I_z) \cos \theta + P(S_z) \sin \theta}{\cos \theta + \sin \theta} \right. \\ &\quad \left. - \cos \beta (2P(2I_z S_z) + (P(S_z) - P(I_z)) \tan 2\theta) \right) \\ a_{3 \rightarrow 1} &= \frac{1}{8} \sin \beta (1 - \sin 2\theta) \left( 2 \frac{P(I_z) \cos \theta - P(S_z) \sin \theta}{\cos \theta - \sin \theta} \right. \\ &\quad \left. + \cos \beta (2P(2I_z S_z) + (P(S_z) - P(I_z)) \tan 2\theta) \right) \end{aligned} \quad (16)$$

Thus the signal amplitudes depend on the nutation angle  $\beta$ , on the parameter  $\theta$  that describes the strength of the coupling, and on  $P(I_z), P(S_z)$ , and  $P(2I_z S_z)$ .

### 2.5. Asymmetry of doublets

In practice, if the violation of the high temperature approximation is significant, e.g., if  $P(^{13}\text{C}') > 5\%$ , one can experimentally observe an asymmetry  $A_S$  of the doublet of the spy nucleus  $S$  coupled to the spin  $I$  under investigation, even in weakly coupled systems ( $\theta = 0$ ), provided that a pulse with a nutation angle  $\theta \neq 90^\circ$  is used. This asymmetry can differ dramatically from the ‘‘roof effect’’ usually observed at thermal equilibrium.

Even without calibration or *a priori* knowledge of the signal integrals (i.e., without prior measurement of the thermal equilibrium signal), the amplitude of the anti-phase component can be normalized with respect to the amplitude of the in-phase component as follows:

$$A_S = \frac{a_{2 \rightarrow 1} - a_{4 \rightarrow 3}}{a_{2 \rightarrow 1} + a_{4 \rightarrow 3}} \quad (17)$$

This normalized asymmetry can be expressed as follows by combining Eqs. (16) and (17):

$$A_S = \frac{P(2I_z S_z) + \sin 2\theta (aP(S_z) + bP(I_z))}{P(S_z)(c+a) - P(I_z)(c-b) + P(2I_z S_z) \sin 2\theta} \quad (18)$$

where  $a = (\cos 2\theta + \cos \beta) / (2 \cos \beta \cos 2\theta)$ ,  $b = (\cos 2\theta - \cos \beta) / (2 \cos \beta \cos 2\theta)$ , and  $c = \cos 2\theta ((1 - \cos \beta) / (2 \cos \beta))$ .

At first glance, the asymmetry  $A_S$  results in a complex mixture of numerous terms, but as pointed out by Lau et al. [13] the measured asymmetry according to Eq. (17) ‘correlates strongly’ with the polarization  $P(I_z)$ .

Two simple limits may be considered: (1) the high temperature approximation where  $P(2I_z S_z) = 0$  and  $P(I_z) = P(S_z)$ ; and (2) the limit for weak coupling when  $\theta \rightarrow 0$ . These cases lead to greatly simplified equations:

$$\lim_{\Delta E/kT \rightarrow 0} A_S = \sin 2\theta \quad (19)$$

$$\lim_{\theta \rightarrow 0} A_S = \cos \beta \cdot \frac{P(2I_z S_z)}{P(S_z)} \quad (20)$$

Keeping in mind that  $\theta$  is negative if  $J_{IS} < 0$  or  $\Delta v < 0$ , we shall demonstrate in the following section that under some assumptions related to the DNP process and to nuclear spin–lattice relaxation after dissolution, the measured asymmetry  $A_S$  does in fact properly reflect the absolute polarization  $P(I_z)$ .

### 2.6. Low temperature DNP and uniform spin temperature

In dissolution DNP, the polarization generally builds up at low temperatures (typically between 1.2 and 4.2 K) and moderate fields (often between 3.35 and 6.7 T). The characteristic time constant  $\tau_{\text{DNP}}$  of the DNP build-up can range from a few minutes to hours, much longer than the time required for spin-diffusion to establish a uniform nuclear spin polarization in the sample. Unless the radicals and/or analytes have very low concentrations or have an unusual inhomogeneous distribution, the assumption of a uniform nuclear spin polarization or temperature appears fully justified.

### 2.7. Initial DNP polarizations

If a uniform spin temperature  $T_{\text{spin}}$  is established in the solid state by DNP prior to dissolution, i.e., if the two spins  $I$  and  $S$  have the same spin polarizations  $P(I_z) = P(S_z) = P_0$ , the distribution of the populations at time  $t = 0$  immediately after dissolution can be described by a Boltzmann distribution. If, without loss of generality, the energy of the eigenstates  $\phi_2$  and  $\phi_3$  are set to zero, one obtains

$$\begin{aligned} n_1^{\text{DNP}} &= \frac{e^{+\hbar\omega/kT}}{Z} \\ n_2^{\text{DNP}} &= n_3^{\text{DNP}} = \frac{1}{Z} \\ n_4^{\text{DNP}} &= \frac{e^{-\hbar\omega/kT}}{Z} \end{aligned} \quad (21)$$

where  $Z = e^{-\hbar\omega/kT} + 2 + e^{+\hbar\omega/kT} = (e^{-\hbar\omega/2kT} + e^{+\hbar\omega/2kT})^2$

The nuclear spin polarizations generated by DNP can be expressed:

$$\begin{aligned}
P(I_z)_0 &= P(S_z)_0 = \frac{e^{+\hbar\omega/kT} - e^{-\hbar\omega/kT}}{(e^{+\hbar\omega/2kT} + e^{-\hbar\omega/2kT})^2} \\
&= \frac{(e^{+\hbar\omega/2kT} + e^{-\hbar\omega/2kT})(e^{+\hbar\omega/2kT} - e^{-\hbar\omega/2kT})}{(e^{+\hbar\omega/2kT} + e^{-\hbar\omega/2kT})^2} \\
&= \frac{(e^{+\hbar\omega/2kT} - e^{-\hbar\omega/2kT})}{(e^{+\hbar\omega/2kT} + e^{-\hbar\omega/2kT})} = \tanh(\hbar\omega/2kT) = P_0 \quad (22)
\end{aligned}$$

$$\begin{aligned}
P(2I_z S_z)_0 &= \frac{e^{+\hbar\omega/kT} - 2 + e^{-\hbar\omega/kT}}{(e^{+\hbar\omega/2kT} + e^{-\hbar\omega/2kT})^2} = \frac{(e^{+\hbar\omega/kT} - e^{-\hbar\omega/kT})^2}{(e^{+\hbar\omega/2kT} + e^{-\hbar\omega/2kT})^2} \\
&= \tanh^2(\hbar\omega/2kT) = P_0^2 \quad (23)
\end{aligned}$$

## 2.8. Initial asymmetry and polarization at time $t = 0$

Assuming that the polarization enhanced by DNP could be entirely preserved during dissolution, transfer and injection into the sample tube that is waiting in the NMR or MRI system, the initial asymmetry  $A_{S,0}$  would take a simple form obtained by combining Eqs. (18), (22) and (23):

$$A_{S,0} = P_0 \cos \beta \frac{1 + \sin 2\theta / (P_0 \cos \beta)}{1 + \sin 2\theta \cdot P_0 \cos \beta} \quad (24)$$

which can be reorganized as follows:

$$P_0 = \frac{A_{S,0}}{\cos \beta} \cdot \frac{1 - \sin 2\theta / A_{S,0}}{1 - \sin 2\theta \cdot A_{S,0}} \quad (25)$$

Thus the polarization can be readily determined from the initial asymmetry provided the nutation angle  $\beta$  and the angle  $\theta$  that describes the strength and sign of the coupling are known.

## 2.9. Relaxation after dissolution

In reality, dissolution and transfer from the polarizer to the NMR or MRI magnet may take several seconds. In this interval, the sample may be exposed to a time-dependent magnetic field  $B_0(t)$  although the variations may be smoothed out by using a 'magnetic tunnel' [24]. During the transfer, the decay and partial interconversion of the two-spin order and the Zeeman terms are determined by coupled relaxation [25]:

$$\frac{d}{dt} \begin{bmatrix} \Delta(I_z) \\ \Delta(S_z) \\ \Delta(2I_z S_z) \end{bmatrix} = - \begin{bmatrix} \rho_I & \sigma_{SI} & \delta_{ISI} \\ \sigma_{IS} & \rho_S & \delta_{ISS} \\ \delta_{ISI} & \delta_{ISS} & \rho_{IS} \end{bmatrix} \cdot \begin{bmatrix} \Delta(I_z) \\ \Delta(S_z) \\ \Delta(2I_z S_z) \end{bmatrix} \quad (26)$$

where  $\Delta(I_z)$ ,  $\Delta(S_z)$ , and  $\Delta(2I_z S_z)$  represent deviations from thermal equilibrium,  $\rho_I$ ,  $\rho_S$ , and  $\rho_{IS}$  represent the decay rates of the two Zeeman order terms (with  $\rho_I = 1/T_1^{(I)}$  and  $\rho_S = 1/T_1^{(S)}$ ) and of the longitudinal two-spin order term,  $\sigma_{SI} = \sigma_{IS}$  represent the coupling between the Zeeman terms, i.e. the cross-relaxation rates that can give rise to Overhauser effects, and  $\delta_{ISI}$  and  $\delta_{ISS}$  represent the 'cross-correlation rates' that couple the Zeeman terms with the longitudinal two-spin order term. These rates can be expressed using the notation of Fig. 1:

$$\begin{aligned}
\rho_I &= W_2 + W_0 + W_I^\alpha + W_I^\beta \\
\rho_S &= W_2 + W_0 + W_S^\alpha + W_S^\beta \\
\rho_{IS} &= W_I^\alpha + W_I^\beta + W_S^\alpha + W_S^\beta \\
\sigma_{IS} &= \sigma_{SI} = W_2 - W_0 \\
\delta_{ISI} &= W_I^\alpha - W_I^\beta \\
\delta_{ISS} &= W_S^\alpha - W_S^\beta
\end{aligned} \quad (27)$$

As a general rule, both cross-relaxation and cross-correlation rates tend to drive the asymmetry  $A_S$  towards values that may

significantly differ from  $P(I_z)$ . If these relaxation pathways can be neglected, the relaxation matrix (26) is diagonal:

$$\frac{d}{dt} \begin{bmatrix} \Delta(I_z) \\ \Delta(S_z) \\ \Delta(2I_z S_z) \end{bmatrix} \cong - \begin{bmatrix} \rho_I & 0 & 0 \\ 0 & \rho_S & 0 \\ 0 & 0 & \rho_I + \rho_S \end{bmatrix} \cdot \begin{bmatrix} \Delta(I_z) \\ \Delta(S_z) \\ \Delta(2I_z S_z) \end{bmatrix} \quad (28)$$

The conditions that must be fulfilled for this approximation to hold are:

$$\begin{aligned}
W_I^\alpha &\approx W_I^\beta \\
W_S^\alpha &\approx W_S^\beta
\end{aligned} \quad (29)$$

and

$$W_2, W_0 \ll W_I^\alpha, W_S^\alpha \quad (30)$$

If the conditions of Eqs. (29) and (30) are fulfilled, the asymmetry  $A_S$  can faithfully reflect  $P(I_z)$  even after dissolution, transfer, injection, and partial relaxation in the NMR or MRI magnet. These conditions hold for  $^{13}\text{C}$  spin pairs, especially when relaxation is driven by intramolecular dipole-dipole interactions with nearby protons, or by external fluctuating fields which may be due to solvent, radicals, dissolved triplet oxygen, or paramagnetic impurities. Violations of these conditions need to be evaluated on a case-by-case basis.

## 2.10. Asymmetry after dissolution

Under the assumptions of Eqs. (29) and (30), one has  $\rho_{IS} = \rho_I + \rho_S$ , so that after an arbitrary time  $t$ , the two-spin order polarization is given by:

$$\begin{aligned}
P(2I_z S_z) &= P_0^2 \cdot e^{-t(\rho_I + \rho_S)} \\
&= (P_0 \cdot e^{-t\rho_I})(P_0 \cdot e^{-t\rho_S}) = P(I_z) \cdot P(S_z)
\end{aligned} \quad (31)$$

And therefore the asymmetry can be written:

$$A_S = \frac{P(I_z) \cdot P(S_z) + \sin 2\theta (a P(S_z) + b P(I_z))}{P(S_z)(c + a) - P(I_z)(c - b) + P(I_z) \cdot P(S_z) \sin 2\theta} \quad (32)$$

Again, it is worth considering two limits:

$$\lim_{\Delta E/kT \rightarrow 0} A_S = \sin 2\theta \quad (33)$$

$$\lim_{\theta \rightarrow 0} A_S = \cos \beta \cdot P(I_z) \quad (34)$$

Eq. (32) can be greatly simplified without loss of generality (error below 2%) by assuming that the main parameters lie within bounds that are usually fulfilled in dissolution-DNP experiments:

- (1) The two nuclear spin polarizations lie in the ranges  $0.01 \leq |P(I_z)| \leq 0.5$  and  $0.01 \leq |P(S_z)| \leq 0.5$ . In practice, the polarization lies in the range between 10% and 20% in most published studies, well above the lower limit of 0.01 (1%). On the other hand, the upper limit  $|P(S_z)| = 0.5 = 50\%$  corresponds to the highest  $^{13}\text{C}$  polarization that can typically be achieved.
- (2) The coupling is weak, i.e.,  $-1^\circ \leq \theta \leq 1^\circ$ , hence  $-0.035 \leq \sin 2\theta \leq 0.035$ , which is indeed valid for most  $^{13}\text{C}$  spin pairs in high fields.
- (3) The nutation angle is small, i.e.,  $-5^\circ \leq \beta \leq 5^\circ$ , which corresponds to standard practice.

Then, if these conditions are fulfilled, the asymmetry can be approximated by the relation:

$$A_S \approx P(I_z) + \sin 2\theta \quad (35)$$

Thus the absolute nuclear spin polarization  $P(I_z)$  of the spin  $I$  under investigation is a function of the asymmetry  $A_S$  of the spy spin  $S$  and the coupling strength expressed by the angle  $\theta$ :

$$P(I_z) \approx A_S - \sin 2\theta \quad (36)$$

### 2.11. Asymmetry in arbitrary two-spin systems

In the previous equations, the asymmetry of  $A_S$  was defined for a coupled two-spin system with  $\gamma_1 > 0$ ,  $\gamma_S > 0$ ,  $J_{IS} > 0$ , and  $|v_S| > |v_I|$ . However, the definition of the asymmetry of  $A_S$  can be extended to all possible cases where  $\gamma_1$ ,  $\gamma_S$ , and  $J_{IS}$  may have arbitrary signs and where one may have  $|v_S| < |v_I|$  while the polarization  $P(I_z)$  induced by DNP may be positive or negative (there are no less than  $2^4 = 16$  different possibilities). To be general, we will define the asymmetry  $A_S$  as a function of the intensities of the high frequency ( $a_{HF}$ ) and low frequency ( $a_{LF}$ ) transitions of the spy spin  $S$ , regardless of its position (chemical shift de-shielded or shielded, i.e., towards higher or lower frequencies) with respect to the investigated spin  $I$  (see Fig. 2):

$$A_S = \frac{a_{LF} - a_{HF}}{a_{LF} + a_{HF}} \quad (37)$$

For a simple homonuclear case where  $\gamma_1 = \gamma_S$  and  $J_{IS} > 0$ , the general case of Eq. (37) agrees with the special case of Eq. (17).

The asymmetry can be approximated in the same manner as in Eq. (35) to obtain a general equation that depends on the signs of  $\gamma_1$ ,  $\gamma_S$ ,  $J_{IS}$  and of the polarization  $P(I_z)$ . Note that the sign of  $\Delta v$  is now simply contained in  $\theta$ , which results in the final equation:

$$A_S \approx s \cdot P(I_z) + \sin 2\theta \quad (38)$$

with

$$s = \frac{J_{IS}\gamma_I\gamma_S}{|J_{IS}\gamma_I\gamma_S|} \quad (39)$$

Note that we have considered the usual coupling constant  $J_{IS}$  rather than the “reduced coupling constant”  $K_{IS} = 4\pi^2 J_{IS}/(h\gamma_I\gamma_S)$ .

Thus,  $P(I_z)$  can be expressed as:

$$P(I_z) \approx s \cdot (A_S - \sin 2\theta) \quad (40)$$

## 3. Results and discussion

Figs. 3 and 4 show  $^{13}\text{C}$  spectra measured with  $\beta = 5^\circ$  pulses immediately after injection of the hyperpolarized solution, for different permutations of the spy and investigated spins  $S$  and  $I$  in singly-enriched  $[1-^{13}\text{C}]\text{pyruvate-}d_3$  and doubly-enriched  $[1,2-^{13}\text{C}_2]\text{acetate-}d_3$ . Deuteration of the pyruvate and acetate molecules provides a way of extending  $^{13}\text{C}$  relaxation times in methyl groups but SPY-MR works equally well in non-deuterated molecules. The  $^{13}\text{C}$  enriched sites can readily be used as spies  $S$  for the determination of the polarization of coupled sites  $I$  even if the latter are in natural abundance. However, on our spectrometer, naturally abundant  $^{13}\text{C}$  sites could only be used as spies  $S$  if the sites  $I$  were enriched. In fact, despite the sensitivity enhancement provided by dissolution-DNP, no signals arising from pairs of coupled spins  $I$  and  $S$  in natural abundance could be measured with our equipment, the probability of such pairs being only about  $10^{-4}$ . All graphs presented in Figs. 3 and 4 show marked asymmetries  $A_S$  that allow one to determine the polarizations  $P(I_z)$  of coupled spins. The experimental spectra were fitted using Matlab. The polarizations  $P(I_z)$  were systematically deduced from the asymmetries  $A_S$  and compared with the corresponding thermal equilibrium signals after complete relaxation in the traditional way described above. Table 1 shows the polarizations  $P(I_z)$  in  $[1-^{13}\text{C}]\text{pyruvate-}d_3$

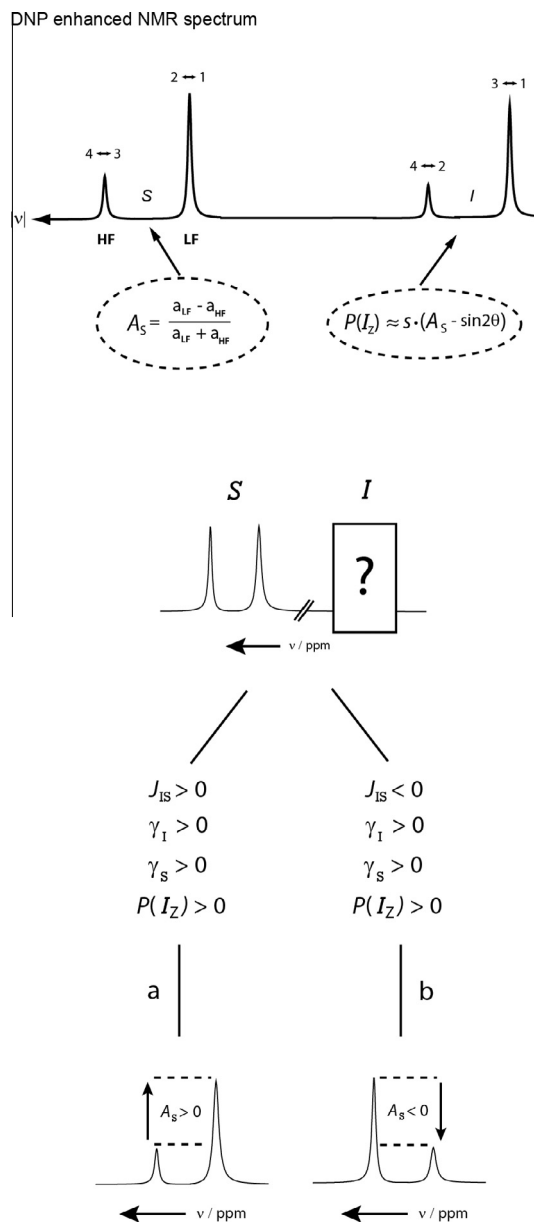
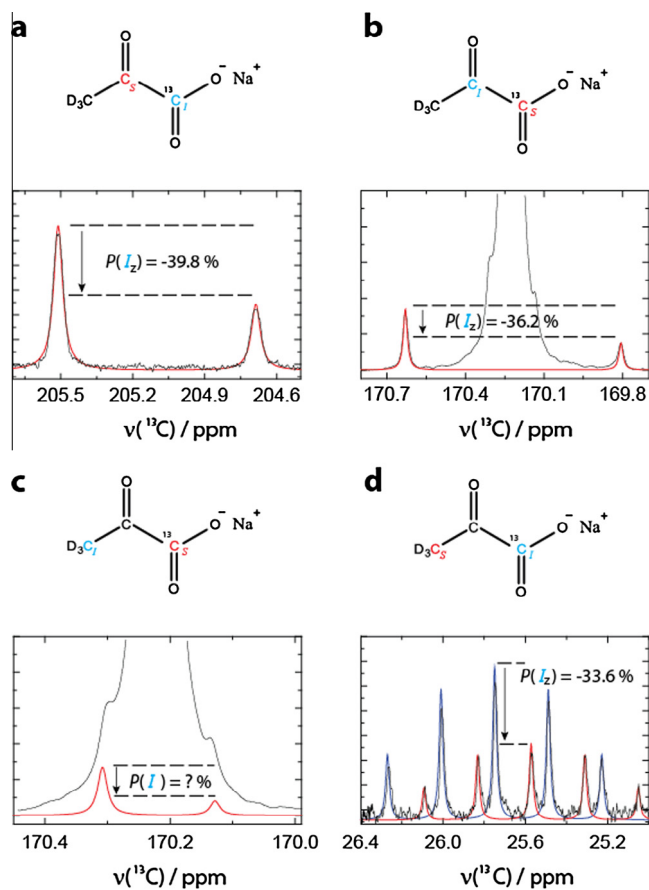


Fig. 2. Illustration of an NMR spectrum of an arbitrary pair of coupled spins  $I$  and  $S$  enhanced by dissolution DNP. Two examples of the  $2^4$  possibilities for a coupled two-spin system are shown with their respective asymmetries. The same pattern as b is obtained if an odd number of the parameters  $\{\gamma_I, \gamma_S, J_{IS}, P(I_z)\}$  has a negative value. Thus the absolute sign of  $J_{IS}$  can readily be determined.

and  $[1,2-^{13}\text{C}_2]\text{acetate-}d_3$  determined both by conventional comparisons of DNP enhanced spectra with their thermal equilibrium equivalents, and by SPY-MR through the asymmetries  $A_S$ .

SPY-MR can provide a rapid measurement of nuclear spin polarizations; however the reliability of the method needs to be evaluated on a case-by-case basis. Table 1 clearly illustrates the fact that for doubly enriched  $[1,2-^{13}\text{C}_2]\text{acetate-}d_3$ , the determination of the two  $^{13}\text{C}$  polarizations is more accurate by SPY-MR than by a conventional comparison with thermal equilibrium measurements, even when the latter are accumulated over ca. 12 h, since the standard deviation can be improved typically by a factor 10. On the other hand, for the singly enriched  $[1-^{13}\text{C}]\text{pyruvate-}d_3$ , the use of SPY-MR is not justified for all combinations of pairs  $S$  and  $I$ . If  $S = ^{13}\text{CO}$  and  $I = ^{13}\text{COO}^-$ , the polarization of the enriched  $^{13}\text{COO}^-$  group can be accurately estimated to be  $P(^{13}\text{COO}^-)$



**Fig. 3.** Asymmetric doublets observed immediately after dissolution-DNP in singly enriched  $[1-^{13}\text{C}]$ pyruvate- $d_3$  using various spy spins  $S$ . The drawings of  $[1-^{13}\text{C}]$ pyruvate- $d_3$  highlight which spins are used as a spies  $C^S$  (red), and which spins  $C^I$  are being investigated (blue). All asymmetries  $A_S < 0$  are negative since the high-frequency (left-hand) doublet components are more intense, corresponding to negative polarizations of investigated spins  $P(I_2) < 0$ . The polarizations estimated by SPY-MR are shown in each spectrum. The following spin pairs  $I$  and  $S$  are shown: (a)  $S = ^{13}\text{CO}$  and  $I = ^{13}\text{COO}^-$  with  $P(^{13}\text{COO}^-) = -39.8 \pm 1\%$  ( $J = 64$  Hz,  $\sin 2\theta = 0.024$ ), (b)  $S = ^{13}\text{COO}^-$  and  $I = ^{13}\text{CO}$  with  $P(^{13}\text{CO}) = -36.2 \pm 2\%$  (with the same  $J = 64$  Hz,  $\sin 2\theta = -0.024$ ), (c)  $S = ^{13}\text{COO}^-$  and  $I = ^{13}\text{CD}_3$  with  $P(^{13}\text{CD}_3)$  undetermined by SPY-MR ( $J = 15$  Hz,  $\sin 2\theta = 0.0014$ ) and (d)  $S = ^{13}\text{CD}_3$  and  $I = ^{13}\text{COO}^-$  with  $P(^{13}\text{COO}^-) = -33.6 \pm 4\%$  (with the same  $J = 15$  Hz,  $\sin 2\theta = -0.0014$ ).

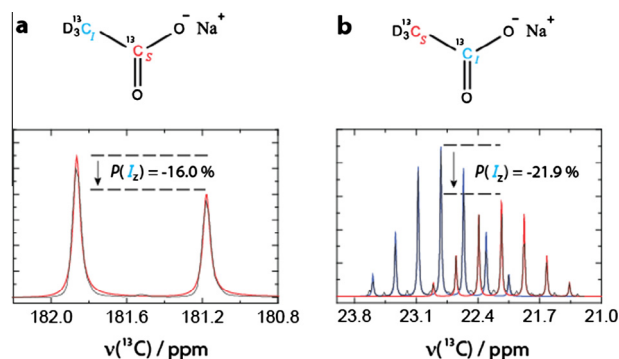


**Fig. 4.** Asymmetric doublets observed immediately after dissolution-DNP in doubly-enriched  $[1,2-^{13}\text{C}]$ acetate- $d_3$  using the same conventions as in Fig. 2. Both asymmetries and polarizations are again negative  $A_S < 0, P(I_2) < 0$ . The following spin pairs  $I$  and  $S$  are shown: (a)  $S = ^{13}\text{COO}^-$  and  $I = ^{13}\text{CD}_3$  with  $P(^{13}\text{CD}_3) = -21.9 \pm 1\%$  ( $J = 53$  Hz,  $\sin 2\theta = -0.0045$ ) and (b)  $S = ^{13}\text{CD}_3$  and  $I = ^{13}\text{COO}^-$  with  $P(^{13}\text{COO}^-) = -16.0 \pm 1\%$  (with the same  $J = 53$  Hz,  $\sin 2\theta = 0.0045$ ).

$= -39.8 \pm 1\%$  (see Fig. 3a). For all others pairs  $S$  and  $I$ , however, SPY-MR gave less accurate results than the conventional thermal equilibrium approach:

1. The polarizations could not be estimated when both  $S$  and  $I$  are in natural abundance for the  $^{13}\text{CO}$  and  $^{13}\text{CD}_3$  spin pair in deuterated pyruvate because of a lack of sensitivity. On the other hand, the traditional thermal equilibrium approach provided estimates  $P(^{13}\text{CO}) = -30.9\%$  and  $P(^{13}\text{CD}_3) = -22.6\%$ , albeit with a limited accuracy of  $\pm 5\%$ .
2. The polarizations of the naturally abundant  $I = ^{13}\text{CO}$  and  $I = ^{13}\text{CD}_3$  spins could be investigated *via* the enriched  $S = ^{13}\text{COO}^-$  spins in deuterated pyruvate, however with a limited accuracy because of the overlap of the satellite lines with the intense central line. This overlap is less severe for  $I = ^{13}\text{CO}$  (see Fig. 3b), giving a reliable estimate of the polarization  $P(^{13}\text{CO}) = -36.2 \pm 2\%$ . However for  $I = ^{13}\text{CD}_3$ , this overlap is more severe (see Fig. 3c) and it is not possible to determine the polarization  $P(^{13}\text{CD}_3)$ . In fact, the satellite lines are hidden under the central peak, and poor shimming or phase errors have detrimental effects on the determination of the  $I$  spin polarization.
3. The polarization of the isotopically enriched  $I = ^{13}\text{COO}^-$  spins could be investigated by observing the naturally abundant  $S = ^{13}\text{CD}_3$  spins, despite the complex pattern arising from couplings to three deuterons (see Fig. 3d). The estimate  $P(^{13}\text{COO}^-) = -33.6 \pm 4\%$  resulting from the observation the spy  $S = ^{13}\text{CD}_3$  is less accurate than  $P(^{13}\text{COO}^-) = -38.9 \pm 1\%$  that could be determined by using the spy  $S = ^{13}\text{CO}$ . Deuterium decoupling could be used to reduce overlap.

As a general rule, even when using state-of-the-art instrumentation, SPY-MR requires at least one of the two sites  $I$  or  $S$  to be enriched. We shall distinguish between three possible scenarios: (a) when both sites are enriched, either site can be used as spy and the determination of the polarization of the other site is straightforward. (b) When only the investigated spin  $I$  is enriched, the spy spin  $S$  in natural abundance gives rise to a doublet (albeit with a nearly 200-fold reduced sensitivity) with an asymmetry  $A_S$  that allows one to determine the polarization  $P(I_2)$ , as illustrated in Fig. 3a and d. (c) When the investigated  $I$  spin is in natural abundance, the spectrum of the enriched spy  $S$  mainly features two weak satellite peaks owing to the 1.1% abundance of  $^{13}\text{C}$  of the site  $I$ . If they can be resolved, their asymmetry allows one to determine the polarization  $P(I_2)$ . However, depending on the line-widths and scalar coupling constants, the intense central peak can overlap with the satellite peaks and affect the accuracy of the SPY-MR approach. This is nicely illustrated in Fig. 3b where the satellites partly overlap with the central peak, and in Fig. 3c where the overlap is so critical that a reliable estimate of the polarization  $P(I_2)$  is difficult.

Fig. 5 shows a comparison of the hyperpolarization decay in the deuterated methyl group ( $^{13}\text{CD}_3$ ) estimated by conventional means and by SPY-MR with the asymmetry ( $A_S$ ) of the neighboring  $\text{COO}^-$  group in acetate. One can see that the asymmetry reliably reflects the absolute polarization until a certain point ( $t \sim 50$  s). After that, the two curves obviously diverge from each other. This can be attributed to small cross-relaxation and cross-correlation rates that can have a significant effect on a timescale longer than  $T_1$ . Moreover, the asymmetry of the  $\text{COO}^-$  peaks becomes increasingly difficult to determine when the signal-to-noise ratio decreases on the course of the decay.

**Table 1**  
Absolute polarization  $P(I_z)$  of various investigated nuclear spins  $I$  in hyperpolarized singly enriched  $[1-^{13}\text{C}]$ pyruvate- $d_3$  and in doubly enriched  $[1,2-^{13}\text{C}]$ acetate- $d_3$ . The polarizations were determined at  $B_0 = 7$  T (300 MHz for protons) and  $T = 298$  K immediately after dissolution, either by a conventional comparison with the corresponding thermal equilibrium signals measured after complete relaxation, or by SPY-MR through the asymmetry of a coupled spy spin. Estimates of the uncertainties in thermal reference spectra were based on their modest signal-to-noise ratios (SNR). In the case of SPY-MR, systematic errors, due to baseline distortions, phase errors, overlapping signals, and other factors are likely to be larger than the errors resulting from noise, since the SNR is very high. The systematic errors were estimated somewhat arbitrarily to be on the order of 1%.

Investigated $^{13}\text{C}$ site $I$	$P(I_z)$ (%) from equilibrium	Spy $^{13}\text{C}$ site $S$	$A_S$ Asymmetry	$\sin 2\theta$ Roof effect	$P(I_z)$ (%) from asymmetry
<i>Pyruvate</i>					
COO	$-32.3 \pm 5$	CO	$-0.374 \pm 0.01$	+0.024	$-39.8 \pm 1$
		CD <sub>3</sub>	$-0.337 \pm 0.04$	-0.0014	$-33.6 \pm 4$
CO	$-30.9 \pm 5$	COO	$-0.386 \pm 0.02$	-0.024	$-36.2 \pm 2$
		CD <sub>3</sub>	N.A.	N.A.	N.A.
CD <sub>3</sub>	$-22.6 \pm 5$	COO	?	+0.0014	?
		CO	N.A.	N.A.	N.A.
<i>Acetate</i>					
COO	$-15.7 \pm 5$	CD <sub>3</sub>	$-0.223 \pm 0.01$	-0.0045	$-21.9 \pm 1$
CD <sub>3</sub>	$-11.6 \pm 5$	COO	$-0.155 \pm 0.01$	+0.0045	$-16.0 \pm 1$

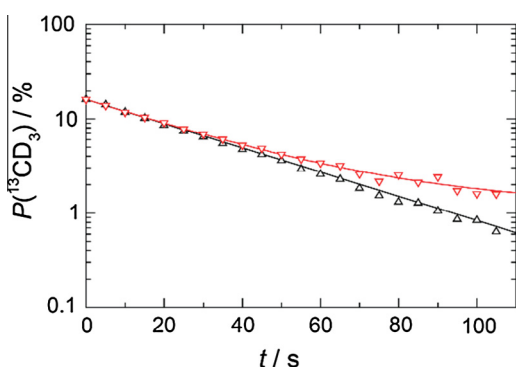


**Fig. 5.** Hyperpolarized decay of  $^{13}\text{CD}_3$  in  $[1,2-^{13}\text{C}]$ acetate- $d_3$  ( $\Delta$ ) obtained from  $T_1$  relaxation measured with  $5^\circ$  nutation angle pulses, and ( $\nabla$ ) derived from the asymmetry  $A_S$  of the neighboring  $\text{COO}^-$  group.

## 4. Experimental

### 4.1. Sample preparation

An amount of 111 mg (1 mmol) of  $[1-^{13}\text{C}]$  sodium pyruvate was added to 20 ml  $\text{D}_2\text{O}$  99.9% (both from Cambridge Isotope Laboratories). The pH of the solution was adjusted to 10 by addition of 10  $\mu\text{l}$  of 1 M NaOD (Sigma–Aldrich). This solution was stirred for 1 day at room temperature. After stopping the reaction with 1 M DCl (Sigma–Aldrich) to make the pH neutral, the extent of the exchange reaction was monitored by  $^1\text{H}$  and  $^{13}\text{C}$  NMR. The solution was lyophilized in order to remove  $\text{D}_2\text{O}$ . A white powder was obtained as final product. Two solutions were prepared in a glass-forming solvent mixture  $\text{D}_2\text{O}:\text{H}_2\text{O}:\text{glycerol-}d_8$  ( $v:v:v = 40:10:50$ ) doped with 50 mM TEMPOL. Sample 1 contained 1.5 M singly-labeled sodium  $[1-^{13}\text{C}]$  pyruvate- $d_3$  and Sample 2 contained 1.5 M doubly-labeled sodium  $[1,2-^{13}\text{C}_2]$ acetate- $d_3$  (Cambridge Isotope Laboratories).

### 4.2. Dissolution-DNP experiments

Of each sample 5 drops of 10  $\mu\text{l}$  were frozen in liquid nitrogen and inserted into our DNP polarizer operating at  $B_0 = 6.7$  T and  $T = 1.2$  K. Five frozen drops of 10  $\mu\text{l}$  each containing 3 M ascorbate in  $\text{D}_2\text{O}$  were also inserted in the polarizer in order to scavenge the radicals after dissolution [26]. DNP was performed by monochromatic microwave irradiation ( $P_{\mu\text{w}} \approx 80$  mW,  $f_{\mu\text{w}} = 188.3$  GHz) and combined with long-range  $^1\text{H} \rightarrow ^{13}\text{C}$  cross-polarization (with CP contacts at intervals of 5 min) from the protons of the  $\text{D}_2\text{O}$ :

$\text{H}_2\text{O}$  mixture to the  $^{13}\text{C}$  nuclei in deuterated  $[1-^{13}\text{C}]$ pyruvate- $d_3$  and  $[1,2-^{13}\text{C}_2]$ acetate- $d_3$  [27]. Dissolution was performed as described elsewhere [28] in 700 ms with 5 mL  $\text{D}_2\text{O}$  preheated to  $T = 400$  K at 1.0 MPa. The dissolved sample was pushed by helium gas at 0.6 MPa in 3.5 s to a 7 T Bruker magnet through a 1.5 mm inner diameter polytetrafluoroethylene (PTFE) tube protected by a 0.9 T magnetic tunnel [24] leading to a home-built injector just above a 5 mm sample tube containing 250  $\mu\text{l}$  of  $\text{D}_2\text{O}$  for field-frequency locking in a 7.05 T magnet (300 MHz for protons). The sample was then injected in *ca.* 2 s. The complete sequence of dissolution, transfer, and injection takes about 6.2 s. A series of  $5^\circ$  pulses were then applied to the  $^{13}\text{C}$  nuclei at intervals of 5 s.

### 4.3. Relaxation matrix

The SPY-MR method was applied to  $^{13}\text{C}$  spin pairs in hyperpolarized solutions of sodium pyruvate and acetate. Since for  $^{13}\text{C}$  spin pairs the main relaxation mechanisms stem from external interactions such as those due to paramagnetic oxygen, free radicals, or other nuclei (inter- or intra-molecular dipolar interactions with other nuclear spins), Eqs. (33) and (34) are satisfied. Consider the pair of  $^{13}\text{C}$  spins of the carboxyl and carbonyl nuclei in pyruvate. The relaxation matrix was determined as follows: (i) the crystal structure of sodium pyruvate was obtained from the Cambridge Structural Database, (ii) the CSA tensor was predicted with CASTEP [29], and (iii) the relaxation was calculated using the SpinDynamica [30] code for Mathematica. Note that internal dynamics in solution may alter both the effective CSA tensors and rates. The relaxation matrix was found to be:

$$\begin{bmatrix} \rho_I & \sigma_{SI} & \delta_{ISI} \\ \sigma_{IS} & \rho_S & \delta_{ISS} \\ \delta_{ISI} & \delta_{ISS} & \rho_{IS} \end{bmatrix} \cong -10^{-4} \begin{bmatrix} \mathbf{146} & 2.05 & -1.10 \\ 2.05 & \mathbf{211} & 0.44 \\ -1.10 & 0.44 & \mathbf{352} \end{bmatrix} \quad (41)$$

Clearly, the cross-relaxation and cross-correlation rates are significantly lower than the single-quantum rates  $\rho_I$  and  $\rho_S$ , typically by nearly two orders of magnitude. Thus the relaxation matrix is essentially diagonal, and  $\rho_{IS} \approx \rho_I + \rho_S$ , so that  $\Delta(2I_z S_z)$  decays almost twice as fast as  $\Delta(I_z)$  and  $\Delta(S_z)$ . Therefore, the SPY-MR method can safely be applied to this  $^{13}\text{C}$  spin pair. We shall assume that this is also valid for the  $^{13}\text{C}$  spin pairs in sodium acetate and pyruvate.

## 5. Conclusions

We have shown that SPY-MR can provide an alternative to conventional thermal equilibrium measurements to estimate the

absolute polarization of  $^{13}\text{C}$  spins after dissolution DNP, provided some precautions are taken. The technique is simple and accurate and obviates the need for recording a reference signal at thermal equilibrium, which requires laborious measurements that can typically last about 12 h. SPY-MR is in principle applicable to a broad variety of coupled nuclear spin systems. We have in this article considered homonuclear examples where the spy spin  $S$  and the spin  $I$  under investigation were both  $^{13}\text{C}$  spins, but heteronuclear cases, say when an isolated  $^1\text{H}$  is used as spy  $S$  while a  $^{13}\text{C}$  spin  $I$  is investigated, could also be addressed. Finally SPY-MR could also be used as a means of unambiguously measuring the absolute sign of the coupling constant  $J_{IS}$  by inspection of the multiplet asymmetry.

## Acknowledgments

The authors thank Martial Rey, Anto Barisic, and Dr. Pascal Miéville from EPFL for valuable technical assistance, Cory Widdifield from ENS Lyon for providing the pyruvate CSA tensor prediction, and Jean-Nicolas Dumez from the CNRS in Gif-sur-Yvette for helping us compute the relaxation of pyruvate with Mathematica. This work was supported by the Swiss National Science Foundation (SNSF), the Ecole Polytechnique Fédérale de Lausanne (EPFL), the Swiss Commission for Technology and Innovation (CTI), Bruker BioSpin Switzerland AG, the French CNRS, and the European Research Council (ERC contract “Dilute para-water”).

## References

- [1] J.H. Ardenkjaer-Larsen, B. Fridlund, A. Gram, G. Hansson, L. Hansson, M.H. Lerche, R. Servin, M. Thaning, K. Golman, Increase in signal-to-noise ratio of  $>10,000$  times in liquid-state NMR, *Proc. Natl. Acad. Sci. USA* 100 (2003) 10158.
- [2] A. Pines, J.S. Waugh, M.G. Gibby, Proton-enhanced nuclear induction spectroscopy  $^{13}\text{C}$  chemical shielding anisotropy in some organic solids, *J. Chem. Phys.* 56 (1972) 1776.
- [3] S.R. Hartmann, E.L. Hahn, Nuclear double resonance in rotating frame, *Phys. Rev.* 128 (5) (1962) 2042.
- [4] S. Jannin, A. Bornet, S. Colombo, G. Bodenhausen, Low-temperature cross polarization in view of enhancing dissolution dynamic nuclear polarization in NMR, *Chem. Phys. Lett.* 517 (2011) 234.
- [5] A. Bornet, R. Melzi, S. Jannin, G. Bodenhausen, Cross polarization for dissolution dynamic nuclear polarization experiments at readily accessible temperatures  $1.2 < T < 4.2$  K, *Appl. Magn. Reson.* 43 (2012) 107.
- [6] S. Jannin, A. Bornet, R. Melzi, G. Bodenhausen, High field dynamic nuclear polarization at 6.7 T: Carbon-13 polarization above 70% within 20 min, *Chem. Phys. Lett.* 549 (2012) 99.
- [7] A. Bornet, R. Melzi, A.J.P. Linde, P. Hautle, B. van den Brandt, S. Jannin, G. Bodenhausen, Boosting dissolution dynamic nuclear polarization by cross polarization, *J. Phys. Chem. Lett.* 4 (2013) 111.
- [8] K. Golman, R. in't Zandt, M. Lerche, R. Pehrson, J.H. Ardenkjaer-Larsen, Metabolic imaging by hyperpolarized C-13 magnetic resonance imaging for in vivo tumor diagnosis, *Cancer Res.* 66 (2006) 10855.
- [9] S.J. Nelson, J. Kurhanewicz, D.B. Vigneron, P.E.Z. Larson, A.L. Harzstark, M. Ferrone, M. van Criekinge, J.W. Chang, R. Bok, I. Park, G. Reed, L. Carvajal, E.J. Small, P. Munster, V.K. Weinberg, J.H. Ardenkjaer-Larsen, A.P. Chen, R.E. Hurd, L.-I. Odegardstuen, F.J. Robb, J. Tropp, J.A. Murray, Metabolic imaging of patients with prostate cancer using hyperpolarized  $[1-^{13}\text{C}]$ pyruvate, *Sci. Transl. Med.* 198 (2013) 198ra108.
- [10] M.E. Merrit, C. Harrison, W. Mander, C.R. Malloy, D.A. Sherry, Dipolar cross-relaxation modulates signal amplitudes in the  $^1\text{H}$  NMR spectrum of hyperpolarized  $^{13}\text{C}$ formate, *J. Magn. Reson.* 189 (2007) 280.
- [11] J. Tropp, Multiplet asymmetry and multi-spin order in liquid-state NMR spectra of hyperpolarized compounds, *Proc. Intl. Soc. Mag. Reson. Med.* 18 (2010) 1026.
- [12] M.C.D. Tayler, I. Marco-Rius, M.I. Kettunen, K.M. Brindle, M.H. Levitt, G. Pileio, Direct enhancement of nuclear singlet order by dynamic nuclear polarization, *J. Am. Chem. Soc.* 134 (2012) 7668.
- [13] J.Y.C. Lau, A.P. Chen, Y.-P. Gu, C.H. Cunningham, A calibration-based approach to real-time *in vivo* monitoring of pyruvate  $\text{C}_1$  and  $\text{C}_2$  polarization using the  $J_{CC}$  spectral asymmetry, *NMR Biomed.* 26 (2013) 1233.
- [14] I. Marco-Rius, K.M. Brindle, Measuring polarization by  $J_{CC}$ -doublets' asymmetry in hyperpolarized  $[1,2-^{13}\text{C}]$ pyruvate may be distorted by singlet order, in: 55th ENC conference, Boston, 2014.
- [15] J.S. Waugh, O. Gonen, P. Kuhns, Fourier transform NMR at low temperatures, *J. Chem. Phys.* 25 (1956) 261.
- [16] N.S. Sullivan, R.V. Pound, Nuclear-spin-lattice relaxation of solid hydrogen at low temperatures, *Phys. Rev. A* 6 (1972) 1102.
- [17] C.M. Edwards, D. Zhou, N.S. Sullivan, Unusual low-temperature effects on the NMR line shapes in solid hydrogen, *Phys. Rev. B* 34 (1986) 6540.
- [18] P. Khuns, O. Gonen, J.S. Waugh, Proton spin-spin and spin-lattice relaxation in  $\text{CaSO}_4 \cdot x \text{H}_2\text{O}$  below 1 K, *J. Magn. Reson.* 82 (1989) 231.
- [19] A. Abragam, M. Chapellier, J.F. Jacquinot, M. Goldman, Absorption lineshape of highly polarized nuclear spin systems, *J. Magn. Reson.* 10 (1973) 322.
- [20] N.N. Kuzma, P. Håkansson, M. Pourfathi, R.K. Ghosh, H. Kara, S.J. Kadlecik, G. Pileio, M.H. Levitt, R.R. Rizi, Lineshape-based polarimetry of dynamically-polarized  $^{15}\text{N}_2\text{O}$  in solid-state mixtures, *J. Magn. Reson.* 234 (2013) 90.
- [21] K. Datta, D. Spielman, Time evolution of  $[1,2-^{13}\text{C}]$ Pyruvate doublet asymmetry in hyperpolarized  $^{13}\text{C}$  MRS, in: ISMRM 23rd Annual Meeting and Exhibition, Toronto, 2015, pp. 4595.
- [22] K.J. Donovan, A. Lupulescu, L. Frydman, Heteronuclear cross-relaxation effects in the NMR spectroscopy of hyperpolarized targets 15 (2014) 436.
- [23] S. Schäublin, A. Höhener, R.R. Ernst, Fourier spectroscopy of nonequilibrium states, application to CIDNP, Overhauser experiments and relaxation time measurements, *J. Magn. Reson.* 13 (1974) 196.
- [24] J. Milani, B. Vuichoud, A. Bornet, P. Miéville, R. Mottier, S. Jannin, G. Bodenhausen, A magnetic tunnel to shelter hyperpolarized fluids, *Rev. Sci. Instrum.* 86 (2015) 024101.
- [25] C. Dalvit, G. Bodenhausen, Proton chemical shift anisotropy: detection of cross-correlation with dipole-dipole interactions by double-quantum filtered two-dimensional NMR exchange spectroscopy, *Chem. Phys. Lett.* 161 (1989) 554.
- [26] P. Miéville, P. Ahuja, R. Sarkar, S. Jannin, P.R. Vasos, S. Gerber-Lemaire, M. Mishkovsky, A. Comment, R. Gruetter, O. Ouari, P. Tordo, G. Bodenhausen, Scavenging free radicals to preserve enhancement and extend relaxation times in NMR using dynamic nuclear polarization, *Angew. Chem. Intern. Ed.* 49 (2010) 6182.
- [27] B. Vuichoud, J. Milani, A. Bornet, R. Melzi, S. Jannin, G. Bodenhausen, Hyperpolarization of deuterated metabolites via remote cross-polarization and dissolution dynamic nuclear polarization, *J. Phys. Chem. B* 118 (2014) 1411.
- [28] A. Comment, B. van den Brandt, K. Uffmann, F. Kurdzesau, S. Jannin, J.A. Konter, P. Hautle, W.T.H. Wenckebach, R. Gruetter, J.J. van der Klink, Design and performance of a DNP prepolarizer coupled to a rodent MRI scanner, *Concepts Magn. Reson. B* 31B (2007) 255.
- [29] S.J. Clark, M.D. Segall, C.J. Pickard, P.J. Hasnip, M.J. Probert, K. Refson, M.C. Payne, First principles methods using CASTEP, *Zeitschrift für Kristallographie* 220 (2005) 567.
- [30] Some of the work in this article employed the SpinDynamica code for Mathematica, programmed by Malcolm H. Levitt, with contributions from Jyrki Rantaharju, Andreas Brinkmann, and Soumya Singha Roy, available at [www.SpinDynamica.soton.ac.uk](http://www.SpinDynamica.soton.ac.uk).